

Higher-Order Sliding Mode Control Scheme with an Adaptation Low for Uncertain Power DC–DC Converters

Amel Hadri-Hamida

Received: 16 September 2014 / Revised: 16 December 2014 / Accepted: 6 January 2015 / Published online: 22 January 2015
© Brazilian Society for Automatics–SBA 2015

Abstract In this paper, a higher-order sliding mode controller for a power DC–DC converter is proposed. The uncertainty and disturbance are implicit to be unknown. A detailed analysis to explore the local and global stability of a Buck DC–DC converter was presented in this paper. Different control schemes were implemented to regulate the output voltage and to eliminate the high current ripples for the proposed converter, beginning with a proportional-integral-derivative compensation scheme, then a sliding mode controller, a higher-order sliding mode controller and finally an adaptation low with higher-order sliding mode controller (AHOSMC). Stability and robustness of the AHOSMC are proved by using the classical Lyapunov criterion. The sensitivity of parameters variation is analyzed, and a detailed bifurcation analysis is undertaken.

Keywords Higher-order sliding mode control · Adaptive higher-order sliding mode control · Bifurcations · DC–DC converters

List of Symbols

T_r	Controlled switch (IGBT)
D	Uncontrolled switch (diode)
L	Inductor
C	Capacitor
R	Load resistance
r_L	Equivalent series resistance of L
r_c	Equivalent series resistance of C
i_L	Inductor current

K_p, T_i, T_d	Parameters of the PID controller
r	Degree of the sliding surface
I_s	Load current
T_{Req}	Equivalent control
H_v	Sensor gain for the output voltage
V_{ref}	Reference voltage
k	Entire number
ϑ	Positive definite matrix
k_1	Positive gain
V_e	Input voltage
V_C	Output capacitor voltage
V_{rc}	Voltage drop across r_C
V_s	Output voltage (the sum of V_C and V_{rc})
α	Duty ratio
T	Switching cycle
F	Switching frequency
T_R	Switching function which can equal to 1 or 0, the control law
S	Sliding surface
λ	Strictly positive constant
K	Positive constant
T_{Rn}	Stabilizing control
H_i	Sensor gain for the inductor current
i_{ref}	Reference current
σ	Sliding function
v	Control law
V	Lyapunov function

1 Introduction

High-frequency and high-power converters are necessary in DC–DC conversion (Tan et al. 2004a, b). However, increasing the switching frequency leads to significant switching losses, which can deteriorate all system efficiency. A huge

A. Hadri-Hamida (✉)
LMSE Laboratory, Department of Electrical Engineering, University of Biskra, 07000 Biskra, Algeria
e-mail: am_hadri@yahoo.fr

step in DC–DC converter technology was taken when the DC link converter was invented (Tan et al. 2005). Stable pulse width modulation (PWM) DC–DC converters are deemed necessary. This leads to analyze the bifurcation pattern of these converters. This PWM DC–DC converter not only has to meet the characteristics demanded by the load, but also must process energy with high efficiency, high reliability, high-power density and low cost (Tan et al. 2006; Hadri Hamida et al. 2006).

The bifurcation analysis denotes for a change in the number of candidate operating conditions of a nonlinear system when a parameter is quasi-statically varied (Tse and Adams 1992; Hadri-Hamida and Allag 2009; Nayfeh and Balachandran 1995). The parameter being varied is referred to as the bifurcation parameter (bp). A nonlinear dynamical system can exhibit many different kinds of bifurcations as one or more parameters are varied.

In its simplest terms, the operation of DC–DC converter can be described as an orderly repetition of a fixed sequence of circuit topologies. The conversion function of the converter is determined by the constituent topologies and the order in which they are repeated (Middlebrook and Cuk 1997; Venkataramanan et al. 1985).

The major difficulty, in the analysis and modeling of PWM DC–DC converters, lies in the fact that the manner in which the system operates is highly nonlinear (Mazumder et al. 2001; Maity et al. 2007). To date, most analytic techniques of modeling and analysis of these converters implement linear feedback systems (Rosehart and Cañizares 1999).

In most of the above investigations, sampled data models or maps of the converters have been derived, and the bifurcation structures have been investigated with the discrete models. Using an exact formulation based on nonlinear maps (Wiggins 1990), we develop a systematic method to model PWM DC–DC converters operating with feedback control.

Here, we have investigated the behavior of the Buck PWM DC–DC converter in the instability zones to shed light on its associated bifurcation with the help of the software package MATLAB (Wang et al. 2000).

To improve the performances of the PWM DC–DC converter, a control strategy based on AHOSMC is proposed, which gives the good performance robust to disturbances as well as the fast transient responses.

The SMC is one of the popular strategies to deal with uncertain control systems (Deane and Hamill 1990). The main feature of SMC is the robustness against parameter variations and external disturbances. Various applications of SMC have been conducted, such as robotic manipulators, aircrafts, DC motors, chaotic systems, and so on (Mattavelli et al. 1993).

The reference Tsang and Chan (2008) presented a model-based cascade controller for DC–DC Buck converters. A dead band relay is introduced in the voltage loop to improve

the disturbance rejection and speed of response of the Buck converter which is modified into an uncertain linear model in Tsai and Chen (2007). Then, SMC technology is adopted to suppress the input disturbance and reduce the effects from the load variation.

In Li et al. (2013), an improved SMC method for a modular multilevel high-voltage DC converter is presented. It merges the merits of the PID neural network and can solve the chattering problem that exists in conventional SMC on-line. The hysteresis modulation SMC is designed in Ramash Kumar and Jeevananthan (2012) for the inherently variable structure of the negative-output elementary boost converter by using a state-space average-based model. In Das and Mahanta (2014), the problem of driving stability for a hybrid vehicle is discussed. The vehicle stability control is addressed using HOSMC and observation techniques. Comparing these works with our work, the contribution of this paper is to apply an AHOSMC to an uncertain Buck DC–DC converter.

We first show that it is feasible to apply a PID feedback control technique to such a system that is operated in high-frequency regimes. Also, the effect of parameter perturbation on the control performance is investigated. In order to eliminate the bifurcations and steady-state error, an SMC control is also introduced to the exact feedback control law. The goal of the first-order SMC is to force the state trajectories to move along the sliding manifold. In the HOSMC, the purpose is to move the states along the switching surface and to keep its order successive time derivatives by using a suitable discontinuous control action. In the AHOSMC, the time derivative of the control input would be designed to act on the higher-order derivatives of the sliding variable (Utkin and Young 1978). Hence, the time derivative of the control would be used as the control input. The new control would be designed as a discontinuous signal, but its integral would be continuous for the eliminating of the high-frequency chattering. It is shown via simulation results that the AHOSMC has high performance both in the transient and in steady-state operations. A good control of the output voltage is obtained.

2 System Model Development

A power circuit of a high-frequency Buck DC–DC converter is introduced in Fig. 1. From the detailed analysis of the PWM Buck converter presented in Hadri-Hamida et al. (2014), we deduce the following large-signal continuous-time system:

$$\begin{cases} \dot{\bar{x}} = \left(\begin{bmatrix} -\frac{1}{L} \left(r_L + \frac{r_C \times R}{r_C + R} \right) & -\frac{1}{L} \left(\frac{R}{r_C + R} \right) \\ \frac{1}{C \times (r_C + R)} & -\frac{1}{C \times (r_C + R)} \end{bmatrix} \bar{x} + \begin{bmatrix} \frac{1}{L} \\ 0 \end{bmatrix} \bar{V}_e \right) \alpha \\ \quad + \left(\begin{bmatrix} -\frac{1}{L} \left(r_L + \frac{r_C \times R}{r_C + R} \right) & -\frac{1}{L} \left(\frac{R}{r_C + R} \right) \\ \frac{1}{C \times (r_C + R)} & -\frac{1}{C \times (r_C + R)} \end{bmatrix} \bar{x} + \begin{bmatrix} 0 \\ 0 \end{bmatrix} \bar{V}_e \right) (1 - \alpha) \\ \bar{V}_s = \left(\begin{bmatrix} \frac{r_C \times R}{r_C + R} & \frac{R}{r_C + R} \end{bmatrix} \alpha + \begin{bmatrix} \frac{r_C \times R}{r_C + R} & \frac{R}{r_C + R} \end{bmatrix} (1 - \alpha) \right) \bar{x} \end{cases} \quad (1)$$

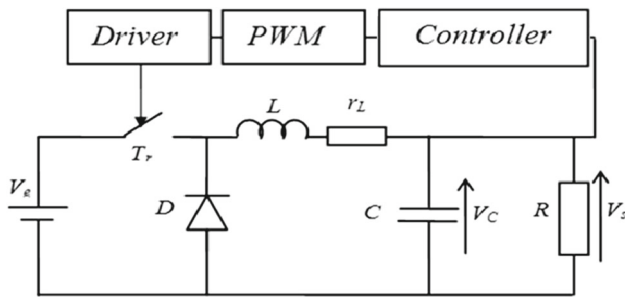


Fig. 1 High-frequency buck DC–DC converter

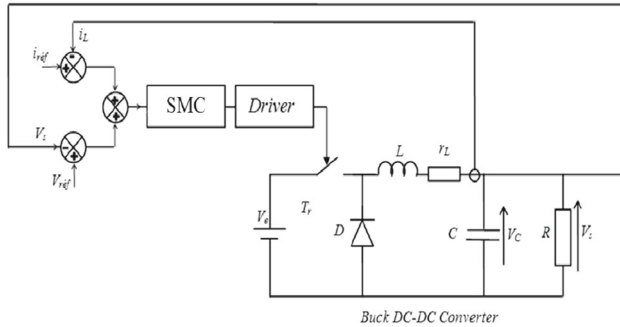


Fig. 2 Closed-loop DC–DC buck converter with SMC

where $x = [i_L, V_C]^T$.

3 Design of the Feedback Control

In this section, different linear and nonlinear controllers are designed for Buck DC–DC converter.

3.1 PID and SMC Controllers

Control applications of PWM DC–DC converters have been widely investigated (Mondal and Mahanta 2011; Utkin et al. 1999; Hadri Hamida et al. 2013; Dong and Tang 2014). The main objective of research and development in this field is always to find the most suitable control method to be implemented in various DC–DC converter topologies. In other words, the goal is to select a control method capable of improving the efficiency of the converter, lessening the effect of electromagnetic interference (EMI), and being less effected by component variation which is the main objective in this work. The bloc scheme in Fig. 2 gives the configuration of the DC–DC Buck converter which utilizes a controller based on a SMC law. The analysis of the PID and the SMC controllers is presented in Appendix.

3.2 Higher-Order Sliding Mode Controller

The objective of the synthesis of a higher-order sliding mode control is to force the trajectories of the system (22) to move

in a finished time on the whole sliding surfaces with a defined order r by:

$$S^r = \left\{ x \in R^n \mid S = \dot{S} = \dots = S^{r-1} = 0 \right\} \quad (2)$$

The r th-order derivative of $S(x)$ satisfies the following equation:

$$S^r(x) = EE(x) + QQ T_R \quad (3)$$

where the matrices $EE(x)$ and $QQ(x)$ are the derivatives of the smooth functions in (29). The r th-order sliding mode control of system (22) with respect to the sliding variable $S(x)$ can be expressed as Benbouzid et al. (2014):

$$\begin{cases} \dot{z}_i = z_{i+1} \\ \dot{z}_r = EE(x) + QQ(x) T_R \end{cases} \quad (4)$$

where $1 \leq i \leq r - 1$, and $[z_1 z_2 \dots z_r]^T = [S(x) \dot{S}(x) \dots S^{r-1}(x)]^T$. By taking the first-order time derivative of (29), we obtain:

$$\begin{aligned} \ddot{S} &= \dot{E}(x) + \dot{Q} T_R + Q \dot{T}_R \\ &= EE(x, T_R) + Q \dot{T}_R \end{aligned} \quad (5)$$

where

$$\begin{aligned} EE &= \left(\frac{H_i}{LC} - \frac{H_i r_L^2}{L^2} + \frac{H_v r_L}{LC} \right) i_L + \left(\frac{H_v}{LC} - \frac{H_i r_L}{L^2} \right) V_C \\ &\quad - \frac{H_i}{LC} I_s + \left(\left(\frac{H_i r_L}{L^2} - \frac{H_v}{LC} \right) V_e \right) T_R. \end{aligned}$$

Finally, the new control law is given by:

$$\dot{T}_R = -Q^{-1} EE(x, T_R) \quad (6)$$

3.3 Adaptive Higher-Order Sliding Mode Controller

Our objective is to design an adaptive HOSMC for use with a Buck DC–DC converter having parameter but unknown R load. With z as the state variable, and from Defoort et al. (2009), the r th-order sliding mode control for system (22) can be written as:

$$\begin{cases} \dot{z}_i = z_{i+1} + \Delta f_i(z, t) \\ \dot{z}_r = EE_n(z) + QQ_n(z) T_R + \Delta f_r(z, t) \end{cases} \quad (7)$$

where $\Delta f(z, t) = \Delta EE(z) + \Delta QQ(z) T_R$, which are the uncertain parts of the matrices $EE(z)$ and $QQ(z)$, and $EE_n(z)$, $QQ_n(z)$ are the nominal parts of matrices $EE(z)$ and $QQ(z)$ respectively.

Assuming $y_1 = S(z)$ and $y_2 = \dot{S}(z)$, the system dynamics can be written as [Mondal and Mahanta \(2013\)](#)

$$\begin{cases} \dot{y}_1 = y_2 \\ \dot{y}_2 = \Phi(z, T_R) + \Psi(z) v \end{cases} \quad (8)$$

where $\Phi(z, T_R) = \dot{E}E_n(z) + \dot{Q}Q_n(z)T_R + \Delta f(z, t)$, $\Psi(z) = QQ_n(z)$, and $v = \dot{T}_R$. Thus, the new control input of the system (8) to be determined becomes v . The sliding function for system (8) is considered as:

$$\sigma = y_2 + K y_1 \quad (9)$$

The derivative of (9) is obtained as:

$$\dot{\sigma} = \dot{y}_2 + K \dot{y}_1 \quad (10)$$

Now, we consider the sliding surface suggested by [Defoort et al. \(2009\)](#)

$$S(z) = z_n - z_n(0) \quad (11)$$

where $z_n(0)$ is the initial condition of the system. The time derivative of (11) is:

$$\dot{S}(z) = \dot{z}_n = EE_n(z) + QQ_n(z)T_R + \Delta f(z, t) \quad (12)$$

and consequently:

$$\ddot{S}(z) = \dot{E}E_n(z) + \dot{Q}Q_n(z)T_R + QQ_n(z)\dot{T}_R + \Delta \dot{f}(z, t) \quad (13)$$

From Eqs. (10), (12), and (13) we can obtain:

$$\begin{aligned} \dot{\sigma} &= \dot{E}E_n(z) + \dot{Q}Q_n(z)T_R + QQ_n(z)\dot{T}_R + \Delta \dot{f}(z, t) \\ &\quad + K(EE_n(z) + QQ_n(z)T_R + \Delta f(z, t)) \\ &= \Phi(z, T_R) + \Psi(z)v + K(\dot{z}) \end{aligned} \quad (14)$$

The control goal is to regulate the voltage source V_C and to reduce the impact of load and component variation ([Zhang et al. 2015](#)) with the elimination of the high current ripple. The new control law becomes:

$$v = -\Psi^{-1}(z) \{ \Phi(z, T_R) + K(\dot{z}) - \dot{\sigma} \} \quad (15)$$

After the use of the constant plus proportional reaching law from [Utkin and Young \(1978\)](#), we obtain:

$$\dot{\sigma} = -\rho \sigma - \delta \text{sign}(\sigma) \quad (16)$$

where $\rho \geq 0$, and $\delta = \frac{1}{R} - \frac{1}{R_n}$. Since δ is unknown, we replace it by its estimate $\hat{\delta} = \frac{1}{\hat{R}} - \frac{1}{R_n}$, we can rewrite

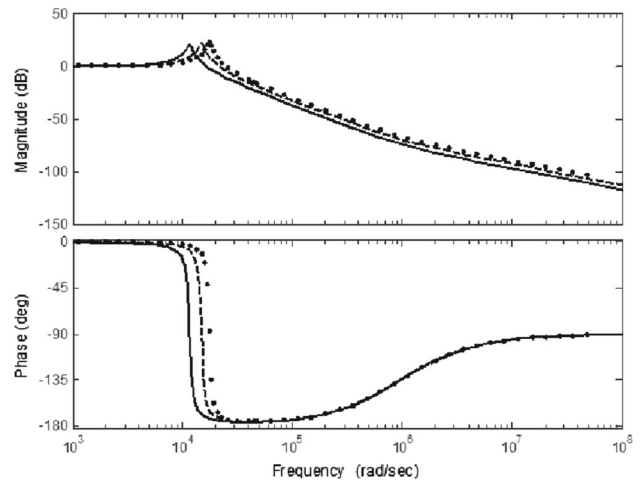


Fig. 3 Frequency response analysis of the converter for $V_e = 18(-), 24(-), 40 V(\dots)$ respectively

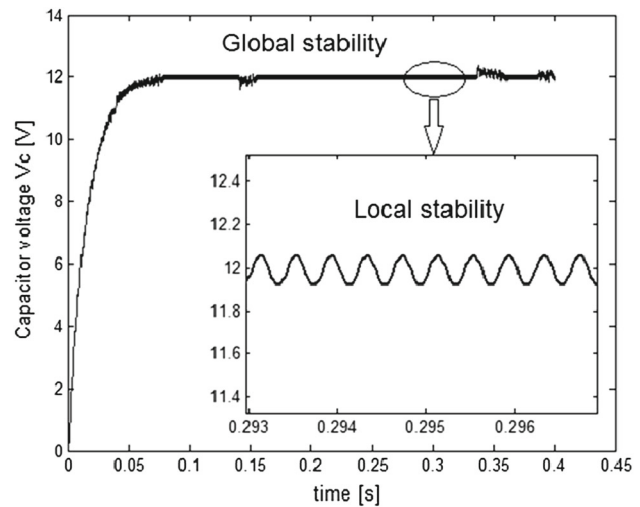


Fig. 4 The asymptotic behavior of a system

equation (15) in a form that suggests an adaptive scheme for the estimation of R load:

$$v = -\Psi^{-1}(z) \{ \Phi(z, T_R) + K(\dot{z}) + \rho \sigma + \hat{\delta} \text{sign}(\sigma) \} \quad (17)$$

We can determine by simulation the poles that give good performance. By using MATLAB Control System Toolbox, one can obtain the gain k_1 . We define the adaptation error e which satisfies:

$$\dot{e} = k_1 e + W_1 \Delta \delta + W_2 \dot{\hat{\delta}} \quad (18)$$

where $\Delta \delta = \frac{1}{R} - \frac{1}{\hat{R}}$ is the error estimate. The existence of the nonlinear term $W_2 \dot{\hat{\delta}}$ suggests the use of the concept of augmented error σ which puts (18) in a familiar form. We introduce the signal ε satisfying ($\dot{\varepsilon} = k_1 \varepsilon + W_2 \dot{\hat{\delta}}$, $\varepsilon(0) = 0$) and the augmented error σ by ($\sigma = e - \varepsilon$) which satisfies $\dot{\sigma} = k_1 \sigma + W_1 \Delta \delta$. We choose the candidate Lyapunov function

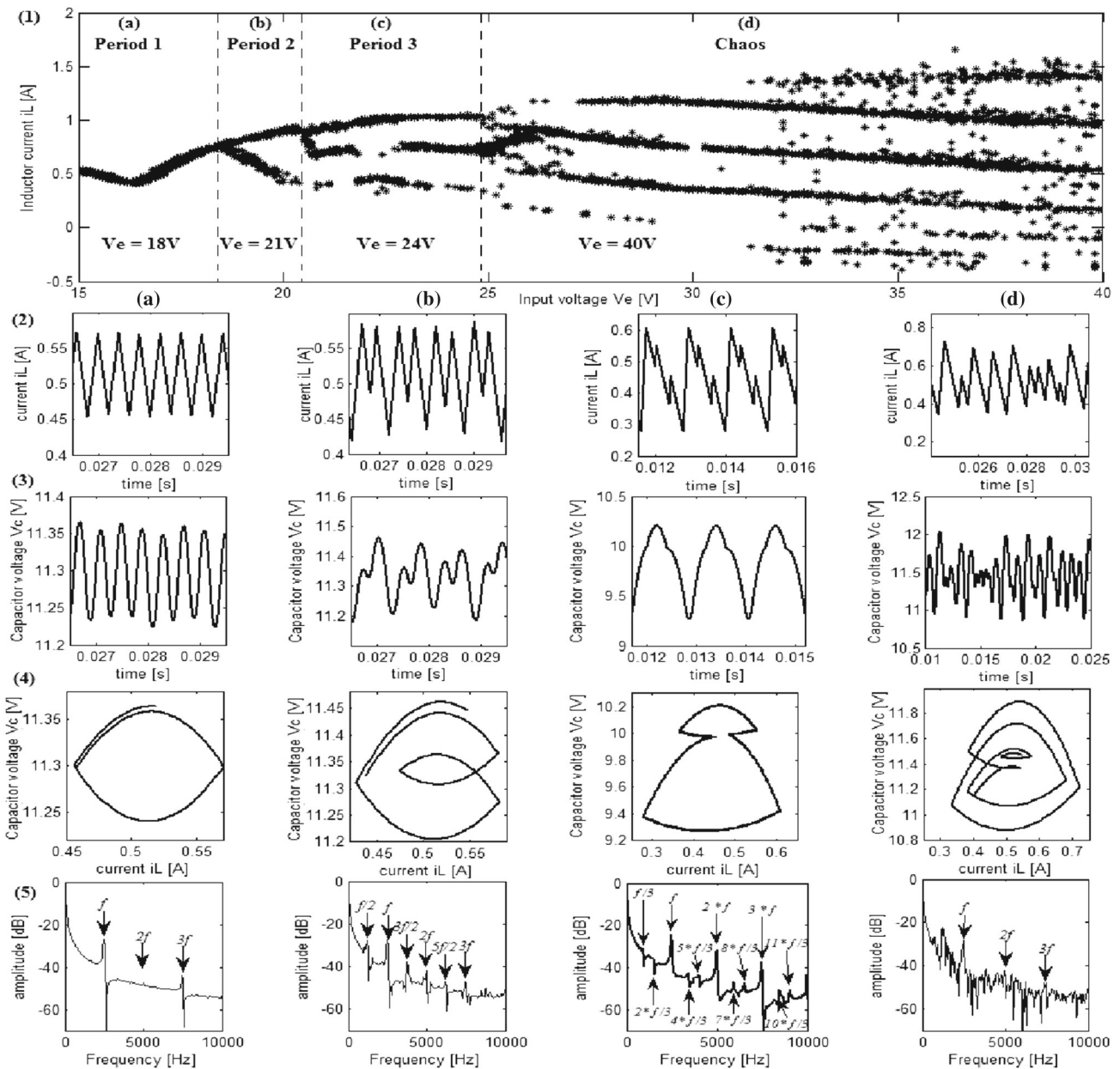


Fig. 5 Steady states of the closed-loop system with a PID controller for different values of V_e , (1) Bifurcation diagram where V_e is the bp, (2) i_L , (3) V_C , (4) state plane and (5) power spectral density of the inductor current

$V = \sigma^T P \sigma + \Delta \delta^T \Gamma \Delta \delta$, and then, we differentiate it, we have:

$$\dot{V} = \sigma^T (k_1^T P + P k_1) \sigma + 2 \Delta \delta^T (W^T P \sigma \Gamma \Delta \delta) \quad (19)$$

In defining the parameter update law under the form $\dot{\delta} = -\Gamma^{-1} W^T P \sigma$, we can guarantee that $\dot{V} = -\sigma^T Q \sigma \leq 0$ where $P = P^T > 0$ is the solution of Lyapunov equation:

$$k_1^T P + P k_1 = -\vartheta \quad (20)$$

Using a standard Lyapunov agreement, we can show that the augmented error $\sigma \rightarrow 0$ as $t \rightarrow \infty$ and that the state z and the error $\Delta \delta$ remain bounded. Considering ϑ as an identity matrix and k_1 , then one can find the solution of Equation (19).

4 Simulation Results

We plot in Fig. 3 the loop gain of the closed-loop regulator system with a PID controller for different values of the input

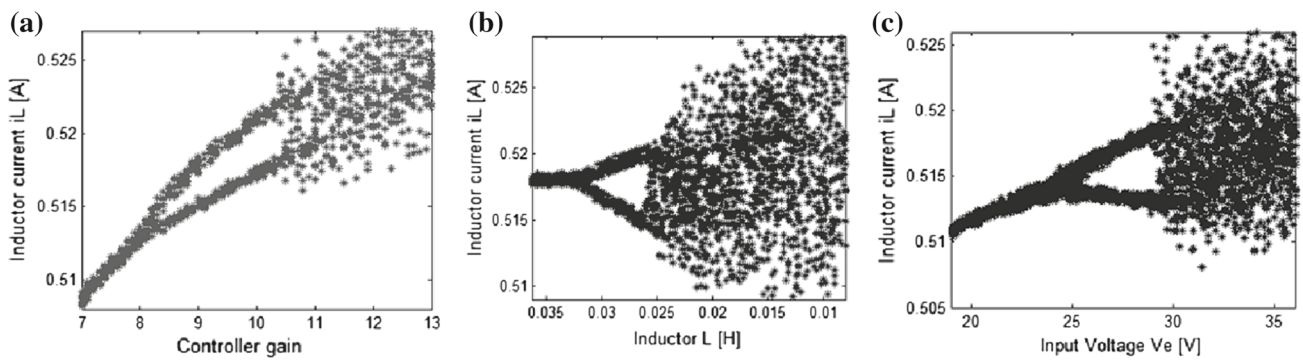


Fig. 6 Bifurcation diagrams. **a** controller gain is the bp, **b** L is the bp, **c** V_e is the bp

Fig. 7 Bifurcation diagram, R is the bp. **a** with PID controller, **b** with SMC

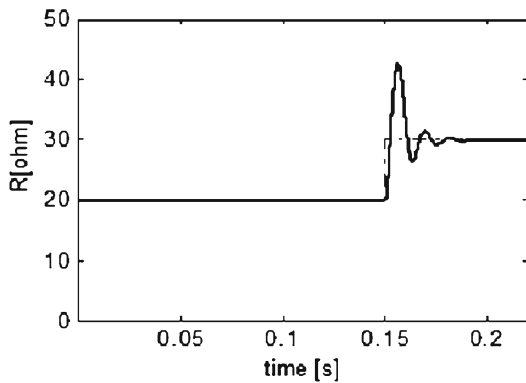
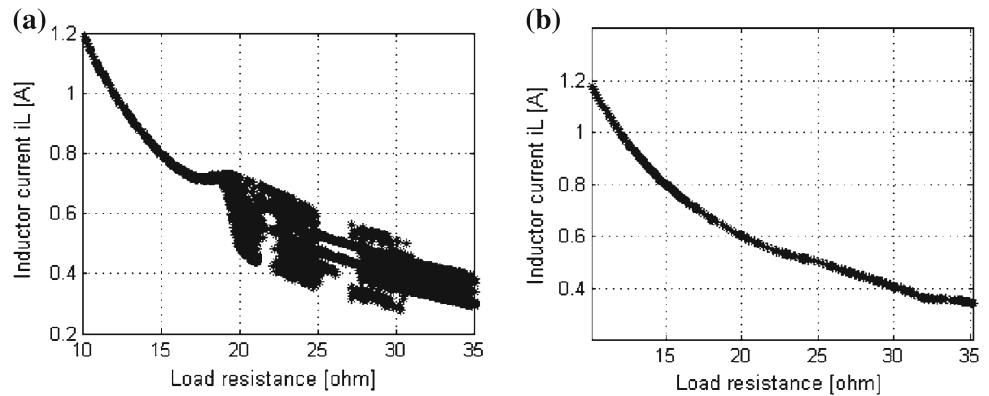


Fig. 8 Estimation of R load

voltage. Even when the input voltage varied, the asymptotic behavior of the converter is overall stable (see Fig. 4) according to the frequency response analysis. In the other hand, in Fig. 5(1), we show the bifurcation diagram with the input voltage as a bp where the converter is not stable locally. The period-one orbit of the closed-loop system is stable. When $V_e = 18$ V, the period-one orbit becomes unstable and a stable period-two orbit emerges. The period-doubling bifurcation was ascertained by computing the Floquet multipliers of the map. When $V_e = 21$ V, the period-two orbit becomes unstable and a period 3 emerges. After the period-three bifur-

cation, the period-three orbit directly bifurcates into a chaotic orbit ($V_e > 40$ V). Next, we present in Fig. 5(2–5) the steady-state waveforms of the closed-loop system with a PID controller applying $V_e = 18, 21, 24,$ and 40 V, respectively. The two-dimensional projections of the phase portraits on the $i_L - V_C$ plane corresponding to these four cases are also shown (Fig. 5(4)). They demonstrate clearly the period 1, period 2, period 3, and chaotic orbits.

The power spectrum density for each of these cases is also shown (Fig. 5(5)). We note that in the case of period 1, appears in the current spectrum an harmonics series of frequency $k * f$ such as k is an entire number, on the other hand, in the case of period 2, the spectrum of the current is enriched with a new series of harmonics of frequency $(k + 0.5) * f$. In period 3, another series of harmonics of frequency $(k/3) * f$ appears in the spectrum of the current, whereas the chaos is appeared by the absence of an ordered series of harmonics.

In Fig. 6, we investigate the effect of the parameter perturbation of the Buck DC–DC converter. These parameters are, respectively, the controller gain, the inductor L , and the input voltage V_e .

The AHOSMC is verified by detailed using MATLAB. A PWM DC–DC model is developed to simulate a switch-on and change load transient conditions, with the control scheme in Fig. 2. In Fig. 7, we show the bifurcation diagram for the system (a) with a PID controller and (b) with an SMC,

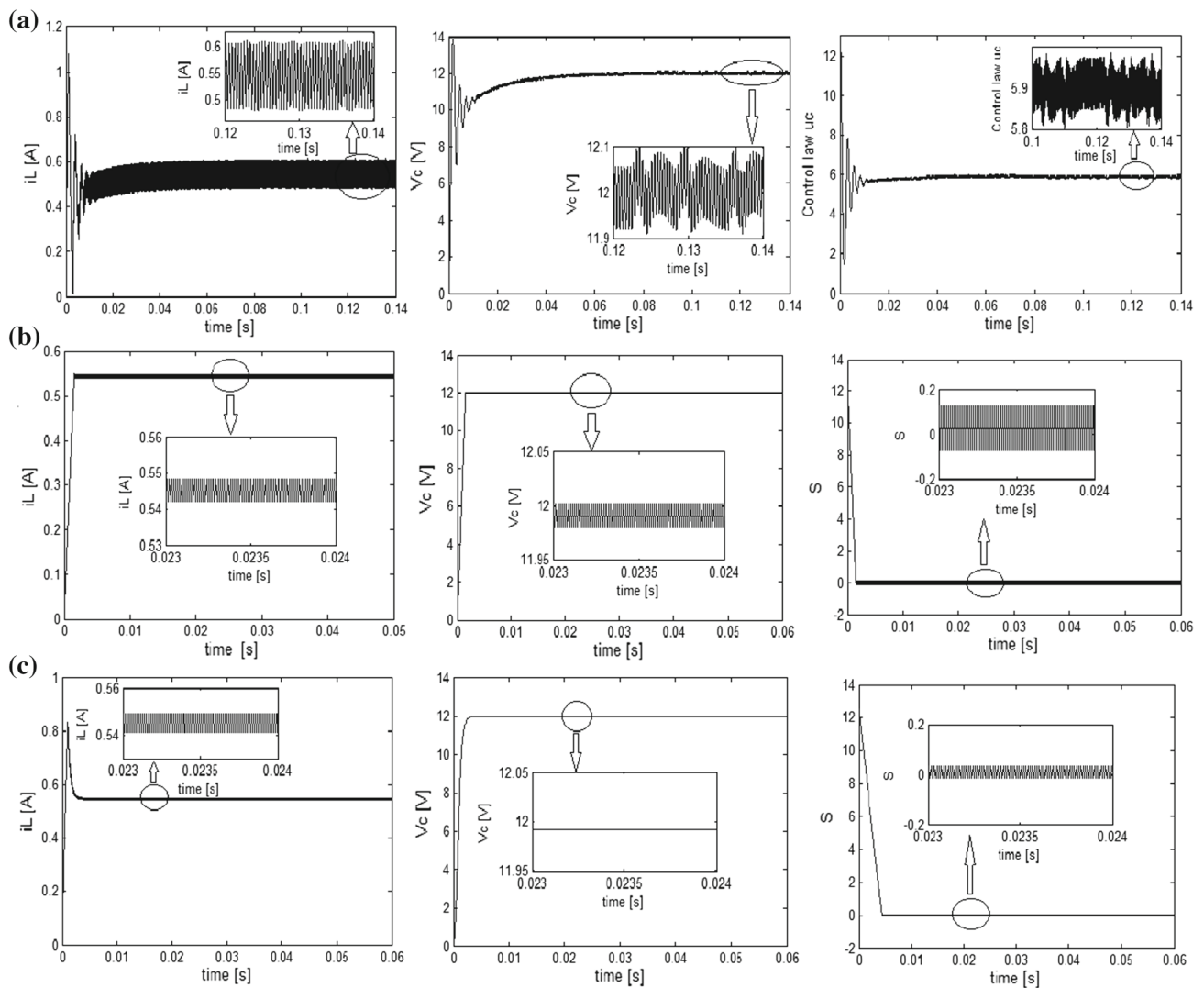


Fig. 9 Inductor current i_L , capacitor voltage V_C , and control law u_c . **a** with PID controller. Inductor current i_L , capacitor voltage V_C , and the sliding surface S . **b** with SMC, **c** with AHOSMC

where the load resistance is the bifurcation parameter. When the load resistance is increased, inductor current decreases, the period-one solution is stable. As R is increased beyond 19Ω , the period-one solution is still stable and the period of the response is not doubled (Fig. 7b). Note that the SMC eliminates the bifurcation of the system orbit. Figure 8 shows the estimation of R load.

From Fig. 9a, we show that the SMC controller ensures finite-time convergence of the system states. However, the high-frequency chattering is always present. In Fig. 9b, the undesired chattering in the current and voltage signal was removed. The dynamic performance of the designed AHOSMC controller is found to be satisfactory compared with that obtained with the conventional SMC and PID controller.

5 Conclusion

In this paper, a nonlinear model was derived for a high-frequency Buck DC–DC converter. The nonlinear model was used to study the stability of this converter. Bifurcation diagrams were generated to study the total behavior of the system as one of its parameters varies.

Next, to improve the performances of our system, we have introduced a sliding mode controller. The results show that the SMC control has fast dynamic response to external disturbances than the PID control and with the SMC control the static and dynamic performances of the output voltage are much better than with the PID control. This technique of control can reduce and sometimes eliminate the effect of load and component variation (bifurcations).

Moreover, a robust model reference AHOSMC is designed in order to diminish the influence of the unknown load uncertainties and disturbances. The advantage of the adaptive HOSMC is translated by the reduction of chattering. The proposed control scheme gives satisfactory simulation results with nominal load.

It is shown through simulation results that the AHOSMC can reduce the internal oscillations, and the performance of the high-frequency Buck DC–DC converter based on AHOSMC scheme is better than the ones based on classical SMC scheme and the PID feedback control scheme.

Appendix

PID and SMC Controllers

We have introduced firstly a PID feedback controller which has the following transfer function:

$$G_{\text{contr}}(p) = k_p \frac{1 + p \cdot T_i + p^2 \cdot T_i \cdot T_d}{p \cdot T_i} \tag{21}$$

Then, we have presented the SMC controller. In SMC, the trajectory of the system is constrained to move or slide along a predetermined hyper plane in the state space. Such mode is completely robust and independent of parametric variations and disturbances (Utkin 1992; Song and Sun 2014). By eliminating the parasitic effect of the capacitor ($r_C = 0$), The system is described by the following state-space equations (Mondal and Mahanta 2013):

$$\begin{cases} \dot{x} = F(x) + G(x, V_e) T_R \\ y = S(x) \end{cases} \tag{22}$$

where the matrices F and G are given by:

$$F(x) = \begin{bmatrix} -\frac{r_L}{L} i_L - \frac{1}{L} V_C \\ \frac{1}{C} i_L - \frac{1}{RC} V_C \end{bmatrix}, \quad G(x, V_e) = \begin{bmatrix} \frac{V_e}{L} \\ 0 \end{bmatrix} \tag{23}$$

And $S(x)$ is the measured output function known as the sliding variable. The general form of $S(x)$ is given as follows (Utkin 1992):

$$S(x) = \left(\frac{d}{dt} + \lambda \right)_x^{r-1} e(x) \tag{24}$$

It is the first convergence condition which permits dynamic system to converge toward the sliding surfaces. It is a question of formulating a positive scalar function $V(x) > 0$ for the system states variables which are defined by the following Lyapunov function (Utkin et al. 1999; Filippov 1964):

$$V(x) = \frac{1}{2} S(x)^T S(x) \tag{25}$$

$$\dot{V}(x) < 0 \Rightarrow S(x)^T \dot{S}(x) < 0 \tag{26}$$

Table 1 Parameters of the buck DC–DC converter (Hadri Hamida 2011)

Input voltage	15 ÷ 50 V
Switching frequency	2.5 * 10 ³ Hz
Inductance	20 * 10 ⁻³ H
Output capacitor	47µF
Equivalent series resistance r_L	0.022 Ω
Equivalent series resistance r_C	0.022 Ω
Load resistance	12 ÷ 35 Ω

Now, we define

$$T_R(t) = \frac{1}{2} (1 + \text{sign}(S)) = T_{Req}(t) + T_{Rn}(t) \tag{27}$$

where $T_{Req}(t)$ and $T_{Rn}(t)$ represent the equivalent control (Utkin 1992) and the nonlinear switching control and:

$$\text{sign}(S) = \begin{cases} 1 & S(x) > 0 \\ -1 & S(x) < 0 \end{cases}$$

The sliding surfaces are given by the following expression (Table 1):

$$S = e(V_s) + e(i_L) = V_{ref} - H_v V_s + i_{ref} - H_i i_L \tag{28}$$

and consequently, their derivatives are given by:

$$\dot{S} = E(x) + QT_R \tag{29}$$

where $x = [i_L \quad V_C]^T$,

$$E = \left(\frac{H_i r_L}{L} - \frac{H_v}{C} \right) i_L + \frac{H_i}{L} V_C + \frac{H_v}{C} I_s,$$

and

$$Q = -\frac{H_i}{L} V_e.$$

Finally, the control law is given by:

$$T_R = -Q^{-1} E(x) + K \text{sign}(S) \tag{30}$$

Parameters of the Buck DC–DC Converter

How to Plot a Bifurcation Diagram?

Let us consider the state equation:

$$\begin{cases} \dot{x} = Ax + BV_e \\ x_0 \end{cases} \tag{31}$$

The diagram of bifurcation of this system is defined in the following way: One represents V_e in X-coordinate (V_e ranging between 15 and 50 V), and we present in ordinate, the values obtained by the solution of the state equation, after a certain iteration count (400 for example). For each value of

V_e , the operation is started again a great number of times by choosing each time a random value of the first term x_0 (equilibrium values). One thus obtains the bifurcation diagram of our system.

References

- Benbouzid, M., Beltran, B., Amirat, Y., Yao, G., Han, J., & Mangel, H. (2014). Second-order sliding mode control for DFIG-based wind turbines fault ride-through capability enhancement. *ISA Transactions*, 53(3), 827–833.
- Das, M., & Mahanta, C. (2014). Optimal second order sliding mode control for nonlinear uncertain systems. *ISA Transactions*, 53(4), 1191–1198.
- Deane, J. H. B., & Hamill, D. C. (1990). Analysis, simulation and experimental study of chaos in the buck converter. In *IEEE proceedings of power electronics*, pp. 491–498.
- Defoort, M., Floquet, T., Kokosyd, A., et al. (2009). A novel higher order sliding mode control scheme. *System & Control Letters*, 58(2), 102–108.
- Dong, L., & Tang, W. C. (2014). Adaptive backstepping sliding mode control of flexible ball screw drives with time-varying parametric uncertainties and disturbances. *ISA Transactions*, 53(1), 110–116.
- Filippov, A. F. (1964). Differential equations with discontinuous right-hand side. *American Mathematical Society Translations*, 42, 199–231.
- Hadri Hamida, A. (2011). Contribution à l'analyse et à la commande des convertisseurs DC–DC parallèles à PWM. Ph.D. Thesis, University of Biskra, Algeria.
- Hadri Hamida, A., Allag, A., Mimoune, S. M., Ayad, M. Y., Becherif, M., Miliani, E., Miraoui, A., & Khanniche, S. (2006). Application of an adaptive nonlinear control strategy to AC–DC–PWM converter feeding induction heating. In *IEEE conference on IECON 2006*, France, pp. 1598–1602.
- Hadri Hamida, A., Zerouali, S., & Allag, A. (2013). Toward a nonlinear control of an AC–DC–PWM converter dedicated to induction heating. In *Frontiers in energy*. Berlin, Heidelberg: Higher Education Press and Springer, vol. 7, no. 2 pp. 140–145.
- Hadri-Hamida, A., Allag, A., et al. (2009). A nonlinear adaptive backstepping approach applied to a three phase pwm AC–DC converter feeding induction heating. *ELSEVIER Journals, Communications in Nonlinear Science and Numerical Simulation*, 14(4), 1515–1525.
- Hadri-Hamida, A., Ghoggal, A., & Zerouali, S. (2014). Bifurcation analysis of a Buck DC–DC converter applied to distributed power systems. *International Journal of System Assurance Engineering and Management, SPRINGER Journals, Sweden*, 5(3), 307–312.
- Li, S., Wang, Z., & Wang, G. (2013). Proportional-integral differential neural network based sliding-mode controller for modular multi-level high-voltage DC converter of offshore wind power. *Electric Power Components and Systems*, 41(4), 427–446.
- Maity, S., Tripathy, D., Bhattacharya, T. K., & Banerjee, S. (2007). Bifurcation analysis of PWM-1 voltage-mode-controlled buck converter using the exact discrete model. *IEEE Transactions on Circuits and Systems*, 54(5), 1120–1130.
- Mattavelli, P., Rossetto, L., Spiazzi, G., & Tenti, P. (1993). General-purpose sliding-mode controller for dc/dc converter applications. In *IEEE Proceedings of PESC*, pp. 609–615.
- Mazumder, S. K., Nayfeh, A. H., & Boroyevich, D. (2001). Theoretical and experimental investigation of the fast- and slow-scale instabilities of a DC–DC converter. *IEEE Transactions on Power Electronics*, 16(2), 201–216.
- Middlebrook, R. D., & Cuk, S. (1977). A general unified approach to modelling switching DC to DC converters in discontinuous conduction mode. In *IEEE power electronic specialists conference*, pp. 36–57.
- Mondal, S., & Mahanta, C. (2013). Adaptive integral higher order sliding mode controller for uncertain system. *Journal of Control Theory Applications CAS and Springer, Berlin, Heidelberg*, vol. 11, no. 1, 61–68.
- Mondal, S., & Mahanta, C. (2011). Nonlinear sliding surface based second order sliding mode controller for uncertain linear systems. *Communications in Nonlinear Science and Numerical Simulation*, 16(9), 3760–3769.
- Nayfeh, A. H., & Balachandran, B. (1995). *Applied nonlinear dynamics*. New York: Wiley.
- Ramash Kumar, K., & Jeevananthan, S. (2012). Analysis, design, and implementation of hysteresis modulation sliding-mode controller for negative-output elementary boost converter. *Electric Power Components and Systems*, 40(3), 292–311.
- Rosehart, W. D., & Cañizares, C. A. (1999). Bifurcation analysis of various power system models. *International Journal of Electrical Power & Energy Systems*, 21(3), 171–182.
- Song, Z., & Sun, K. (2014). Adaptive backstepping sliding mode control with fuzzy monitoring strategy for a kind of mechanical system. *ISA Transactions*, 53(1), 125–133.
- Tan, S. C., Lai, Y. M., Cheung, M. K. H., & Tse, C. K. (2004). An adaptive sliding mode controller for buck converter in continuous conduction mode. In *IEEE proceedings of exposition APEC*, pp. 1395–1400.
- Tan, S. C., Lai, Y. M., Tse, C. K., & Cheung, M. K. H. (2004). A pulse-width modulation based sliding mode controller for buck converters. In *IEEE Proceedings of PESC'04*, pp. 3647–3653.
- Tan, S. C., Lai, Y. M., Cheung, M. K. H., & Tse, C. K. (2005). On the practical design of a sliding mode voltage controlled buck converter. *IEEE Transactions on Power Electronics*, 20(2), 425–437.
- Tan, S. C., Lai, Y. M., Tse, C. K., & Martin, M. K. H. (2006). Adaptive feedforward and feedback control schemes for sliding mode controlled power converters. *IEEE Transactions on Power Electronics*, 21(1), 182–192.
- Tsai, J.-F., & Chen, Y.-P. (2007). Sliding mode control and stability analysis of buck DC–DC converter. *International Journal of Electronics*, 94(3), 209–222.
- Tsang, K. M., & Chan, W. L. (2008). Non-linear cascade control of DC/DC buck converter. *Electric Power Components and Systems*, 36(9), 977–989.
- Tse, C. K., & Adams, K. M. (1992). Quasi-linear modeling and control of DC/DC converters. *IEEE Transactions on Power Electronics*, 7(2), 315–323.
- Utkin, V. I., & Young, K. K. D. (1978). Methods for constructing discontinuity planes in multidimensional variable structure systems. *Automatic Remote Control*, 39, 1466–1470.
- Utkin, V. I. (1992). *Sliding mode in control and optimization*. Berlin: Springer.
- Utkin, V., Guldner, J., & Shi, J. X. (1999). *Sliding mode control in electromechanical systems*. London: Taylor and Francis.
- Venkataramanan, R., Sabanoivc, A., & Cuk, S. (1985). Sliding mode control of DC-to-DC converters. In *IEEE Proceedings of IECON*, pp. 251–258.
- Wang, H. O., Chen, D. S., & Bushnell, L. G. (2000). Dynamic feedback control of bifurcations. In *IEEE proceedings of decision and control*, pp. 1619–1624.
- Wiggins, S. (1990). *Introduction to applied nonlinear dynamical systems and chaos*. New York: Springer.
- Zhang, C., Wang, J., Li, S., Wu, B., & Qian, C. (2015). Robust control for PWM-based DC–DC buck power converters with uncertainty via sampled-data output feedback. *IEEE Transactions Power Electronics*, 30(1).